

# Alpha radioactivity deep-underground as a probe of axion dark matter

Carlo Brogini<sup>a</sup>, Giuseppe Di Carlo<sup>b</sup>, Luca Di Luzio<sup>a</sup>, Claudio Toni<sup>c,a</sup>

<sup>a</sup>*Istituto Nazionale di Fisica Nucleare, Sezione di Padova, Via F. Marzolo 8, 35131 Padova, Italy*

<sup>b</sup>*Istituto Nazionale di Fisica Nucleare, Laboratori Nazionali del Gran Sasso, 67100 Assergi (AQ), Italy*

<sup>c</sup>*Dipartimento di Fisica e Astronomia 'G. Galilei', Università di Padova,  
Via F. Marzolo 8, 35131 Padova, Italy*

---

## Abstract

We propose to investigate the time modulation of radioisotope decays deep underground as a method to explore axion dark matter. In this work, we focus on the  $\alpha$ -decay of heavy isotopes and develop a theoretical description for the  $\theta$ -dependence of  $\alpha$ -decay half-lives, which enables us to predict the time variation of  $\alpha$ -radioactivity in response to an oscillating axion dark matter background. To probe this scenario, we have recently constructed and installed a setup deep underground at the Gran Sasso Laboratory, based on the  $\alpha$ -decay of Americium-241. This prototype experiment, named RadioAxion- $\alpha$ , will allow us to explore a broad range of oscillation's periods, from a micro-second up to one year, thus providing competitive limits on the axion decay constant across 13 orders of magnitude in the axion mass, ranging from  $10^{-9}$  eV to  $10^{-20}$  eV after one month of data collection, and down to  $10^{-22}$  eV after three years.

*Keywords:* Axion dark matter, Alpha decay, Underground physics

---

## 1. Introduction

By addressing the strong CP problem [1, 2, 3, 4] and the dark matter puzzle [5, 6, 7], the Quantum Chromodynamics (QCD) axion provides a compelling pathway beyond the Standard Model of particle physics. In recent years, there has been a flourishing of new experimental strategies for axion detection (for reviews, see e.g. [8, 9, 10]). While traditional approaches to axion searches rely on the model-dependent axion coupling to photons, a remarkable prediction of the QCD axion stems from the model-independent axion coupling to gluons. By promoting the topological  $\theta$ -term of QCD (defined in Eq. (11)) to be a time-varying axion field, one can test the axion-gluon coupling through the oscillating electric dipole moment (EDM) of the neutron, induced by the axion dark matter background [11, 12, 13]. Alternative approaches to constrain the axion-gluon coupling have been discussed e.g. in Refs. [14, 15, 16, 17, 18, 19, 20].

More recently, the authors of Ref. [21] have proposed to look for the time variation of the decay rate of certain radioisotopes, focussing on the  $\theta$ -dependence of  $\beta$ -decay, previously developed in [22]. This enabled them to set bounds on the axion coupling to gluons from Tritium decay, based on data taken at the European Commission's Joint Research Centre [23].

The search for a time dependence of the nuclear decay rates started at the birth of radioactivity science. As a matter of fact, Madame Curie, in her Ph.D. thesis [24], reports on the experiment she conducted to determine the radioactivity of Uranium at midday and midnight, finding no difference between the two determinations. In recent years, several studies have reported a modulation at the per mille level in the decay constants of various nuclei, typically over periods of one year, but also spanning

one month or one day (see Ref. [25] and references therein). Conversely, other researchers have found no evidence of such an effect [23, 26, 27].

To clarify this intricate scenario, we performed a few  $\gamma$ -spectroscopy experiments at the underground Gran Sasso Laboratory [28, 29, 30, 31]. The choice of the underground laboratory is, in our opinion, a key point. Specifically, the rock overburden suppresses the muon and neutron flux by six and three orders of magnitude, respectively. This reduction renders irrelevant the impact of the annual time variation of the cosmic ray flux, which has an amplitude of a few percent [29]. Eventually, we were able to exclude modulations of the decay constant of radioisotopes with amplitudes larger than a few parts per  $10^5$  in  $^{137}\text{Cs}$  [28],  $^{222}\text{Rn}$  [29],  $^{232}\text{Th}$  [30],  $^{40}\text{K}$  and  $^{226}\text{Ra}$  [31], for periods between a few hours and one year.

In this work, we propose to investigate the time modulation of radioisotope decays deep underground as a method to test axion dark matter. Unlike the approach of Ref. [21], we focus on the  $\alpha$ -decay of heavy isotopes and employ a setup designed to explore a much broader range of periods, from a microsecond to one year. From the theoretical side, we have developed a framework for the  $\theta$ -dependence of  $\alpha$ -decay half-lives, allowing us to predict the time variation of  $\alpha$ -radioactivity in response to an oscillating axion dark matter background. On the experimental front, we have constructed and installed a prototype setup (RadioAxion- $\alpha$ ) at the Gran Sasso Laboratory, based on the  $\alpha$ -decay of Americium-241. The choice of  $^{241}\text{Am}$  is motivated by several factors. This isotope has a relatively long half-life of about 432.2 yr (approximately stable on the timescale of the measurement) and it predominantly decays by  $\alpha$ -emission, with a  $\gamma$ -ray byproduct,  $^{241}\text{Am} \rightarrow ^{237}\text{Np} + \alpha + \gamma(59.5 \text{ keV})$ .

The resulting  $\gamma$ -ray can be efficiently detected, using for instance a NaI crystal. Moreover,  $^{241}\text{Am}$  has been produced in nuclear reactors for decades and is easily accessible, often used in ionization-type smoke detectors.

In the following, we present the theoretical framework for the  $\theta$ -dependence of  $\alpha$ -decay and describe the experimental setup that we have installed at the Gran Sasso Laboratory. We conclude with a sensitivity estimate of RadioAxion- $\alpha$  on the axion parameter space and discuss future prospects.

## 2. Microscopic theory of $\alpha$ -decay

We consider a theory of  $\alpha$ -decay of a heavy isotope,  ${}^A_Z\text{X} \rightarrow {}^{A-4}_{Z-2}\text{X} + \alpha$ , obtained by computing the tunnelling probability of the  $\alpha$ -particle within a WKB framework that employs a microscopic  $\alpha$ -daughter-nucleus potential [32, 33, 34]. In the semiclassical approximation, the half-life is calculated as [35, 36]<sup>1</sup>

$$T_{1/2} = \frac{\ln 2}{\nu_0} \exp(K), \quad (1)$$

where, in natural units,

$$K = 2 \int_{r_1}^{r_2} dr \sqrt{2\mu[V_{\text{tot}}(r) - Q_\alpha]} \quad (2)$$

is the WKB integral, with  $\mu = M_\alpha M_d / (M_\alpha + M_d) \approx M_\alpha$  the reduced mass of the  $\alpha$ -daughter-nucleus system,  $Q_\alpha = M(A, Z) - M_d - M_\alpha$  is the energy of the emitted  $\alpha$ -particle and  $r_{1,2}$  the turning points of the potential, defined by the conditions  $V_{\text{tot}}(r_1) = V_{\text{tot}}(r_2) = Q_\alpha$ . In Eq. (1),  $\nu_0$  denotes the assault frequency, i.e. the frequency at which the  $\alpha$ -particle collides against the wall of the potential, which is given by (see e.g. [34])

$$\nu_0 = \frac{1}{2\mu} \left[ \int_0^{r_1} \frac{dr}{\sqrt{2\mu|Q_\alpha - V_{\text{tot}}(r)}} \right]^{-1}. \quad (3)$$

In the limit of a square potential well of depth  $-V_0$  this reads  $\nu_0 = v/(2r_1)$ , with  $v = \sqrt{2(Q_\alpha + V_0)/\mu}$ , which can be interpreted as the frequency at which the  $\alpha$ -particle strikes the barrier [37].

The central potential among the  $\alpha$ -particle and daughter nucleus is the sum of the nuclear potential, the Coulomb potential and the rotational term, i.e.

$$V_{\text{tot}}(\vec{R}) = V_N(\vec{R}) + V_C(\vec{R}) + \frac{\ell(\ell+1)}{2\mu R^2}, \quad (4)$$

where  $\ell$  denotes the angular momentum of the nuclear transition and  $R = |\vec{R}|$ . The nuclear potential is obtained by double-folding the densities of the  $\alpha$  and daughter nucleus [38]

$$V_N(\vec{R}) = \int \int d^3 r_\alpha d^3 r_d \rho_\alpha(\vec{r}_\alpha) \rho_d(\vec{r}_d) \times \tilde{v}(\vec{r} = \vec{r}_d - \vec{r}_\alpha + \vec{R}, \rho_\alpha(\vec{r}_\alpha), \rho_d(\vec{r}_d)), \quad (5)$$

where  $\tilde{v}(\vec{r}, \rho_\alpha, \rho_d) = v(\vec{r}) g(\rho_\alpha, \rho_d)$  is the single-nucleon effective potential with a density-dependent correction. Since for the  $\alpha$ -decay process only the iso-scalar component of the potential contributes, we take as an input the iso-scalar term of the so-called M3Y effective potential, supplemented by a zero-range potential for the single-nucleon exchange [38, 39, 40, 41]

$$\begin{aligned} v_{\text{M3Y}}(\vec{r}) = & \left[ -2134 \frac{\exp(-2.5r)}{2.5r} + 7999 \frac{\exp(-4r)}{4r} \right. \\ & \left. - 276 \delta(\vec{r}) \right] \text{MeV}, \end{aligned} \quad (6)$$

with  $r = |\vec{r}|$  in units of 1 fm  $\approx 1/(198 \text{ MeV})$ . Different choices of the nuclear potential, such as the so-called Paris version of the M3Y potential [42], have a minor impact, with differences at the per mille level in the final result of Eq. (22). For the density-dependent term, we consider [32]

$$g(\rho_\alpha, \rho_d) = (1 - \beta \rho_\alpha^{2/3})(1 - \beta \rho_d^{2/3}), \quad (7)$$

with  $\beta = 1.6 \text{ fm}^2$ . Following Ref. [38], the density distribution for the  $\alpha$  particle has been taken to have the Gaussian form

$$\rho_\alpha(\vec{r}) = 0.4229 \exp(-0.7024r^2) \text{fm}^{-3}, \quad (8)$$

whose volume integral is equal to its mass number  $A_\alpha = 4$ . The matter distribution of the daughter nucleus can be instead described by a spherically symmetric Fermi function [32]

$$\rho(\vec{r}) = \frac{\rho_0}{1 + \exp\left(\frac{r-c_d}{a}\right)}, \quad (9)$$

with  $c_d = r_d(1 - \pi^2 a^2 / (3r_d^2))$ ,  $r_d = 1.13 A_d^{1/3} \text{ fm}$ ,  $a = 0.54 \text{ fm}$ , while  $\rho_0$  is a normalization constant, taken so that the volume integral is equal to the mass number of the daughter particle,  $A_d = A - 4$ .

Finally, the Coulomb potential is given by

$$V_C(\vec{R}) = \begin{cases} \frac{Z_\alpha Z_d \alpha_{\text{QED}}}{2R_c} \left[ 3 - \left(\frac{R}{R_c}\right)^2 \right] & \text{for } R < R_c, \\ \frac{Z_\alpha Z_d \alpha_{\text{QED}}}{R} & \text{for } R > R_c, \end{cases} \quad (10)$$

where  $R_c = c_\alpha + c_d$ , with  $c_\alpha = r_\alpha(1 - \pi^2 a^2 / (3r_\alpha^2))$  and  $r_\alpha = 1.13 A_\alpha^{1/3} \text{ fm}$ .

Within such a framework we are able to reproduce the  $\alpha$ -decay half-lives of heavy isotopes at the order of magnitude level, in accordance with the results of Refs. [32, 33, 34]. Note that the  $\alpha$ -decay process is exponentially sensitive to the WKB integral, so that the lifetimes span several orders of magnitudes when varying the  $Q_\alpha$  value for different nuclei.

## 3. $\theta$ -dependence of $\alpha$ -decay

The  $\theta$ -term of QCD is defined by the operator

$$\mathcal{L}_\theta = \frac{g_s^2 \theta}{32\pi^2} G_{\mu\nu}^a \tilde{G}^{a\mu\nu}, \quad (11)$$

where  $|\theta| \lesssim 10^{-10}$  from the non-observation of the neutron EDM [43]. The smallness of  $\theta$  constitutes the so-called strong

<sup>1</sup>See Ref. [37] for a critical assessment of the WKB formula.

CP problem, which can be solved by promoting the  $\theta$ -term to be a dynamical field,  $\theta \rightarrow a(x)/f_a$ , where  $a(x)$  is the axion and  $f_a$  a mass scale known as the axion decay constant. The axion field acquires a potential in the background of QCD instantons and relaxes dynamically to zero, thus explaining the absence of CP violation in strong interactions [1, 2, 3, 4].

In the following, we will be interested in the  $\theta$ -dependence of nuclear quantities, anticipating the fact that we will interpret  $\theta(t)$  as a time-varying background axion field, related to the dark matter of the universe [5, 6, 7]. The consequences of a non-zero  $\theta$  in nuclear physics have been previously investigated in Refs. [22, 44], also in connection with the idea of establishing an anthropic bound on  $\theta$ .

There are various ways in which the  $\theta$ -dependence can manifest in nuclear physics, the most prominent is through the pion mass [45, 46]

$$M_\pi^2(\theta) = M_\pi^2 \cos \frac{\theta}{2} \sqrt{1 + \varepsilon^2 \tan^2 \frac{\theta}{2}}, \quad (12)$$

with  $M_\pi = 139.57$  MeV and  $\varepsilon = (m_d - m_u)/(m_d + m_u)$ . The  $\theta$ -dependence of other low-lying resonances, including  $\sigma(550)$ ,  $\rho(770)$  and  $\omega(782)$  – which, along with the pion, are responsible for the mediation of nuclear forces in the one-boson-exchange (OBE) approximation – has been determined based on  $\pi\pi$  scattering data in Ref. [47].

A key role for the binding energy of heavy nuclei is played by the  $\sigma$  and  $\omega$  channels, via the contact interactions [48]

$$H = G_S(\bar{N}N)(\bar{N}N) + G_V(\bar{N}\gamma_\mu N)(\bar{N}\gamma^\mu N), \quad (13)$$

which control, respectively, the scalar (attractive) and vector (repulsive) part of the nucleon-nucleon interaction [49, 50]. To describe their  $\theta$ -dependence we employ the following parametrization

$$\eta_S = \frac{G_S(\theta)}{G_S(\theta=0)}, \quad \eta_V = \frac{G_V(\theta)}{G_V(\theta=0)}. \quad (14)$$

In Ref. [51] it was found that the pion mass dependence of  $\omega$  exchange leads to subleading corrections compared to the effects related to the  $M_\pi^2$  sensitivity of the scalar channel. Hence, to a good approximation, we can take  $\eta_V = 1$  and consider only the leading  $\theta$ -dependence in the scalar channel, which is described by the following fit [44] to Fig. 2 in [50]

$$\eta_S(\theta) = 1.4 - 0.4 \frac{M_\pi^2(\theta)}{M_\pi^2}. \quad (15)$$

Moreover, based on the relativistic mean-field simulations of [48] for two specific nuclei, Ref. [50] finds that the variation of the binding energy (BE) for a nucleus of mass number  $A$  can be written as (keeping only the variation due to  $\eta_S(\theta)$ )

$$\text{BE}(\theta) = \text{BE}(\theta=0) + (120A - 97A^{2/3})(\eta_S(\theta) - 1) \text{ MeV}, \quad (16)$$

where the terms proportional to  $A$  and  $A^{2/3}$  represent a volume and surface contribution, in analogy to the semi-empirical mass formula [52]. Note that Eq. (16) can be safely used only in the

small  $\theta$ -value regime, since the underlying nuclear model relies on a strong cancellation between the attractive  $\sigma$  channel and the repulsive  $\omega$  channel.

Hence, substituting the expressions of the BEs above in the definition of  $Q_\alpha = \text{BE}(A-4, Z-2) + \text{BE}(4, 2) - \text{BE}(A, Z)$ , we find

$$Q_\alpha(\theta) = Q_\alpha(\theta=0) - 97 \text{ MeV} (\eta_S(\theta) - 1) \times ((A-4)^{2/3} + 4^{2/3} - A^{2/3}). \quad (17)$$

It turns out that  $Q_\alpha(\theta)$  provides, by far, the leading effect in order to assess the  $\theta$ -dependence of  $\alpha$ -decay.<sup>2</sup> Other possible dependences from  $\theta$  arise from the reduced mass  $\mu$ , see e.g. Eq. (2), and the M3Y nuclear potential. The former is given by  $\mu(\theta) \approx 4m_N(\theta) - \text{BE}_4(\theta)$ , where  $m_N(\theta)$  was computed in Ref. [22], while  $\text{BE}_4(\theta)$  can be read from Eq. (16) with  $A = 4$ . Regarding instead the  $\theta$ -dependence of the M3Y potential, this can be implemented by interpreting the exponential terms in Eq. (6) as arising from  $\sigma$  (attractive) and  $\omega$  (repulsive) exchange in the OBE approximation. Focussing on the leading  $\theta$ -dependence from  $\sigma$  exchange, we can rescale the pre-exponential and exponential factors respectively via  $g_{\sigma NN}^2(\theta)$  and  $M_\sigma^2(\theta)$ . The  $\theta$ -dependence of the  $\sigma$  mass is taken from [22, 47], while the  $\sigma$  coupling can be expressed in terms of  $G_S(\theta) = -g_{\sigma NN}^2(\theta)/M_\sigma^2(\theta)$ . We find that the  $\theta$ -dependence arising from both the reduced mass and the nuclear potential remains always subleading with respect to that from  $Q_\alpha(\theta)$ , basically below the percent level in the final result of Eq. (22). The predominance of the  $\theta$ -dependence of  $Q_\alpha(\theta)$  with respect to that of  $V_{\text{tot}}(\theta)$  in Eq. (2) can be understood by the fact that the WKB integral is defined across the potential barrier, and the latter is dominated by the Coulomb potential that is not affected by  $\theta$ .

#### 4. Axion dark matter time modulation

Assuming an oscillating axion dark matter field from misalignment [5, 6, 7], the time dependence of the  $\theta$  angle can be approximated as  $\theta(t) = \theta_0 \cos(m_a t)$ , with

$$\theta_0 = \frac{\sqrt{2\rho_{\text{DM}}}}{m_a f_a}, \quad (18)$$

in terms of  $\rho_{\text{DM}} \approx 0.45 \text{ GeV/cm}^3$ . For a standard QCD axion, one has

$$m_a f_a = \frac{\sqrt{m_u m_d}}{m_u + m_d} m_\pi f_\pi = (76 \text{ MeV})^2, \quad (19)$$

corresponding to  $\theta_0 = 5.5 \times 10^{-19}$ . In the following, we will treat  $m_a$  and  $f_a$  as independent parameters and discuss the sensitivity of  $\alpha$ -decay observables in the  $(m_a, 1/f_a)$  plane.

Following Ref. [21], we introduce the observable

$$I(t) \equiv \frac{T_{1/2}^{-1}(\theta(t)) - \langle T_{1/2}^{-1} \rangle}{\langle T_{1/2}^{-1} \rangle}, \quad (20)$$

<sup>2</sup>A similar observation was noted in the context of the variation of the fine-structure constant, which impacts primordial nuclear abundances [53].

where  $\langle T_{1/2}^{-1} \rangle$  denotes a time average. Given that the main  $\theta$ -dependence in Eq. (15) arises through the pion mass, we expect that  $T_{1/2}(\theta)$  is analytic in  $\theta^2$  and admits the Taylor expansion<sup>3</sup>

$$T_{1/2}(\theta) \approx T_{1/2}(0) + \dot{T}_{1/2}(0)\theta^2, \quad (21)$$

where we introduced the derivative symbol,  $\dot{f} \equiv df/d\theta^2$ . Since  $\theta^2 \ll 1$ , Eq. (21) does provide an excellent approximation to the full  $\theta$ -dependence, which is anyway taken into account in our numerical analysis. Using  $\langle \cos^2(m_a t) \rangle = 1/2$  and expanding at the first non-trivial order in  $\theta_0$ , we find

$$\begin{aligned} I(t) &\approx -\frac{1}{2} \frac{\dot{T}_{1/2}(0)}{T_{1/2}(0)} \theta_0^2 \cos(2m_a t) \\ &= -4.3 \times 10^{-6} \cos(2m_a t) \left( \frac{\rho_{\text{DM}}}{0.45 \text{ GeV/cm}^3} \right) \\ &\quad \times \left( \frac{10^{-16} \text{ eV}}{m_a} \right)^2 \left( \frac{10^8 \text{ GeV}}{f_a} \right)^2, \end{aligned} \quad (22)$$

where  $\dot{T}_{1/2}(0)/T_{1/2}(0) \approx 125$  has been obtained by fitting the numerical expression of  $T_{1/2}(\theta)$  at small  $\theta$  values. To obtain Eq. (22) we also used  $Q_\alpha(\theta = 0) = 5.486 \text{ MeV}$ , corresponding to the dominant  $\alpha$ -decay transition  $^{241}\text{Am} \rightarrow ^{237}\text{Np}^* + \alpha$  with  $\ell = 0$ , and substituted  $\theta_0$  from Eq. (18). An analytical approximation for  $\dot{T}_{1/2}(0)/T_{1/2}(0)$  valid for the  $\alpha$ -decay of a generic  $^A_Z\text{X}$  isotope is provided in Appendix A.

Note that the large theoretical uncertainty in the prediction of  $T_{1/2}(0)$ , stemming from its exponential dependence from the WKB integral  $K$ , is washed out thanks to the normalization of Eq. (20). In fact, neglecting the small  $\theta$ -dependence arising from  $\nu_0$  in Eq. (3), amounting to an effect below the per mille level in Eq. (22), we have  $\dot{T}_{1/2}(0)/T_{1/2}(0) \approx \dot{K}(0)$ .

## 5. Experimental setup

To study the time modulation of the  $\alpha$ -decay of  $^{241}\text{Am}$ , we built a prototype setup (RadioAxion- $\alpha$ ) which we installed deep underground at the Gran Sasso Laboratory, in a dedicated container. A  $3'' \times 3''$  NaI crystal detects the  $\gamma$ -rays due to the  $\alpha$ -decay of  $^{241}\text{Am}$ , primarily (85% of the time) at 59.5 keV, and the X-rays from  $^{237}\text{Np}$  atomic transitions. The signal from the photomultiplier is processed by an ORTEC digiBASE-E, a 14-pin photomultiplier tube base that is directly connected to the photomultiplier. The digiBASE, the photomultiplier, the crystal and the source, kept in a fixed position in front of the crystal, are closed inside a parallelepiped made of polyethylene, completely surrounded by a passive shielding of 5 cm of copper and 10 cm of lead, in order to suppress the laboratory  $\gamma$ -ray background. Data acquisition operates in list mode, i.e. each signal above the 10 keV threshold is converted to a digital value which is transmitted to the computer along with the time of the event. The time resolution is 160 ns. To mitigate the impact of the digiBASE's quartz aging, we also acquire a signal every second,

<sup>3</sup>This is also verified a posteriori by a numerical fit of the half-life as a function of  $\theta$ .

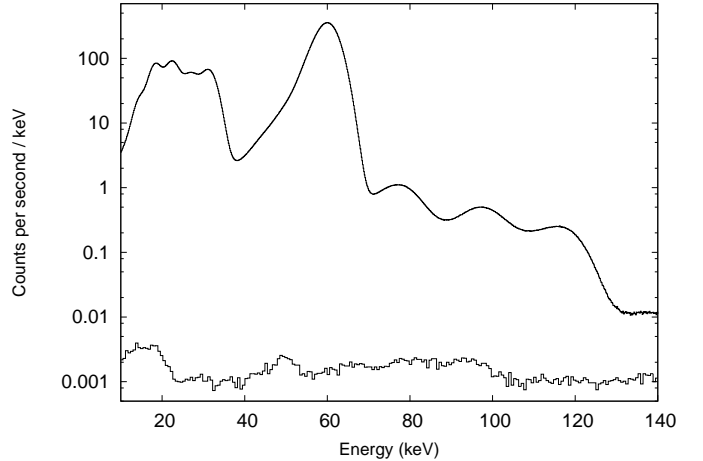


Figure 1:  $\gamma$ -spectrum (counts per second per keV) of the  $^{241}\text{Am}$  source (upper curve) compared to the background (lower curve). The dominant contribution arises from the  $\gamma$  at 59.5 keV.

generated by an FS725 10 MHz Rb Frequency Standard which has a 20 year aging factor of less than  $5 \times 10^{-9}$ .

In Fig. 1 we show the energy spectrum of the events collected in 24 hours, with and without the  $^{241}\text{Am}$  source. With the  $^{241}\text{Am}$  source we have a rate (counts per second) of about 4 kHz, to be compared to a background of 0.2 Hz. The background, i.e. the counts in the absence of the source, is essentially due to the inner radioactivity of the NaI crystal, while the background due to the cosmic ray flux is safely negligible.

## 6. Sensitivity estimate

The theoretical prediction in Eq. (22) can be compared with  $I_{\text{exp}}(t) \equiv (N(t) - \langle N \rangle) / \langle N \rangle$ , where  $N(t)$  is the observed number of events in a given interval of time and  $\langle N \rangle$  its expected value, according to the exponential decay law. Potential sources of systematic errors include the detection of  $\gamma$ -rays and their time-stamping. The former is mitigated by operating the NaI detector well-below the radiation damage threshold and by the reduced background in the underground environment. The latter is handled thanks to the precision of a Rb atomic clock. Hence, we expect our uncertainties to be statistically dominated in the current setup.

We started data taking at the beginning of May 2024. With a rate of about 4 kHz events, we expect to reach a  $2\sigma$  error of  $2 / \sqrt{4000/s \times \pi \times 10^7 s} \approx 6 \times 10^{-6}$  on  $I_{\text{exp}}$  after one year of data taking. Given the 160 ns time resolution of our setup and referring to the oscillation period as  $\Delta t$ , we consider two realistic benchmarks corresponding to distinct experimental phases: *i*) Phase 1:  $1 \mu\text{s} < \Delta t < 10 \text{ days}$  and  $I_{\text{exp}} = 2 \times 10^{-5}$  at  $2\sigma$  with one month of data taking and *ii*) Phase 2:  $1 \mu\text{s} < \Delta t < 1 \text{ yr}$  and  $I_{\text{exp}} = 4 \times 10^{-6}$  at  $2\sigma$  with three years of data taking.

The sensitivity of the present experiment is ultimately limited by the number of detected events due to the  $^{241}\text{Am}$  source. By increasing the source activity by a factor of 10, it would be possible to improve the sensitivity by a factor of 3. Further

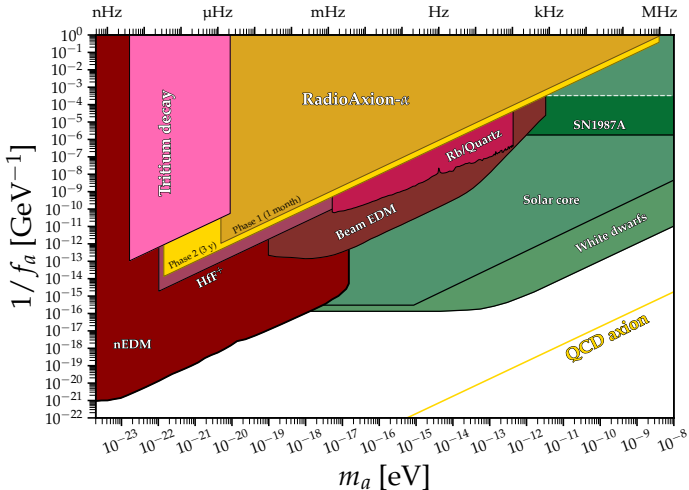


Figure 2: Constraints on the axion dark matter coupling to gluons. The projected sensitivities of RadioAxion- $\alpha$  are displayed for two experimental phases (yellow-shaded areas). Limits from laboratory experiments (red-shaded areas) and astrophysics (green) are shown as well for comparison. Figure adapted from [54].

improvements would require, in addition to a more powerful  $^{241}\text{Am}$  source, a faster detector, for instance a plastic scintillator, and a significantly upgraded data acquisition system. All in all, an improvement of up to two orders of magnitude in the sensitivity could be possible with a set-up similar to ours but with more cutting-edge technologies.

The results of our sensitivity estimate for the two experimental phases of RadioAxion- $\alpha$  are shown in Fig. 2. For comparison, we also display laboratory limits from EDM searches [15, 17, 18], radio-frequency atomic transitions [20], and Tritium decay [21], as well as the SN 1987A bound stemming from the axion-nucleon EDM coupling [11, 55] and finite-density-induced bounds from the solar core and white dwarfs [16, 19]. Note that for  $1/f_a \gtrsim 3.3 \times 10^{-4} \text{ GeV}^{-1}$  (above the dashed line in Fig. 2) axions enter the trapping regime and the cooling bound from SN 1987A does not apply [55].

The yellow, QCD axion line stems from the relationship in Eq. (19), but it remains beyond the reach of the techniques proposed here. The standard  $m_a$ - $f_a$  relation can however be modified in such a way that the axion mass is suppressed for fixed  $f_a$  through a symmetry principle [56, 57, 58, 59]. This can be achieved by employing  $\mathcal{N}$  mirror copies of the Standard Model, endowed with a  $Z_{\mathcal{N}}$  symmetry, under which  $\text{SM}_k \rightarrow \text{SM}_{k+1(\text{mod } \mathcal{N})}$  and the axion acting non-linearly:  $a \rightarrow a + 2\pi k/\mathcal{N}$ , with  $k = 0, \dots, \mathcal{N} - 1$ . It can be shown [56, 57] that this results in the axion mass being exponentially suppressed as  $z^{N/2}$ , with  $z = m_u/m_d \approx 0.5$ , compared to the usual axion mass. Additionally, a modified version of the misalignment mechanism can still support the possibility of axion dark matter [58].

## 7. Conclusions

Our investigation into the time modulation of radioisotope decays deep underground at the Gran Sasso Laboratory has successfully established the RadioAxion- $\alpha$  experiment. This setup,

centered on the  $\alpha$ -decay of  $^{241}\text{Am}$ , will allow us to cover a wide range of oscillation periods from microseconds to a year. Based on realistic projected sensitivities, we will provide with just few years of data competitive constraints on the axion decay constant, spanning 13 orders of magnitude in axion mass, from from  $10^{-9} \text{ eV}$  to  $10^{-22} \text{ eV}$ . We anticipate a better sensitivity compared to existing experiments based on radioactivity, such as Tritium decay, and moderately weaker than radio-frequency atomic transitions, which are both sensitive to  $\theta^2(t)$ . On the other hand, EDM-like searches still remain the most effective ones, since they depend linearly from  $\theta(t)$ .

This work not only marks an additional step in axion dark matter research but also lays the groundwork for a broader project aimed at optimizing the study of the  $\theta$ -dependence of radioactivity. Future efforts will focus on identifying the most effective decay types and isotopes to fully leverage the unique underground environment for axion detection.

## Acknowledgments

We thank Francesco D’Eramo and Massimo Pietroni for discussions at the initial stages of this project, as well as Fabio Zwirner for suggestions on  $\alpha$ -decay theory and Roberto Isocrate for the improvements of the electronics. The work of LDL and CT is supported by the European Union – Next Generation EU and by the Italian Ministry of University and Research (MUR) via the PRIN 2022 project n. 2022K4B58X – AxionOrigins. LDL is also supported by the European Union – NextGeneration EU and by the University of Padua under the 2021 STARS Grants@Unipd programme (Acronym and title of the project: CPV-Axion – Discovering the CP-violating axion).

## Appendix A. Analytical framework for the $\theta$ -dependence of $\alpha$ -decay

In this Appendix we provide an analytical approximation for the  $\theta$ -dependence of  $\alpha$ -decay, parametrized via the factor  $\hat{T}_{1/2}(0)/T_{1/2}(0)$  in Eq. (22), that applies to nuclei with generic values of  $A$  and  $Z$ . In the limit of a squared potential well of depth  $-V_0$ , the total potential reads (assuming  $\ell = 0$ )

$$V_{\text{tot}}(\vec{R}) = \begin{cases} -V_0 & \text{for } R < R_{\text{well}}, \\ \frac{Z_\alpha Z_d \alpha_{\text{QED}}}{R} & \text{for } R > R_{\text{well}}, \end{cases} \quad (\text{A.1})$$

where  $R_{\text{well}}$  is the radius of the well, approximately given by  $R_{\text{well}} \approx R_0 A^{1/3}$ , with  $R_0 \approx 1.13 \text{ fm}$ . Such expression yields the following analytical result for the WKB integral

$$K = Z_\alpha Z_d \alpha_{\text{QED}} \left( \frac{8\mu}{Q_\alpha} \right)^{1/2} F \left( \frac{Q_\alpha R_{\text{well}}}{Z_\alpha Z_d \alpha_{\text{QED}}} \right), \quad (\text{A.2})$$

with

$$F(x) = \arccos \sqrt{x} - \sqrt{x} \sqrt{1-x} \approx \frac{\pi}{2} - 2\sqrt{x} + \dots, \quad (\text{A.3})$$

where in the last step we have considered the  $x \ll 1$  regime, that is typically realized for  $\alpha$ -decay. Note that the factor  $V_0$  drops

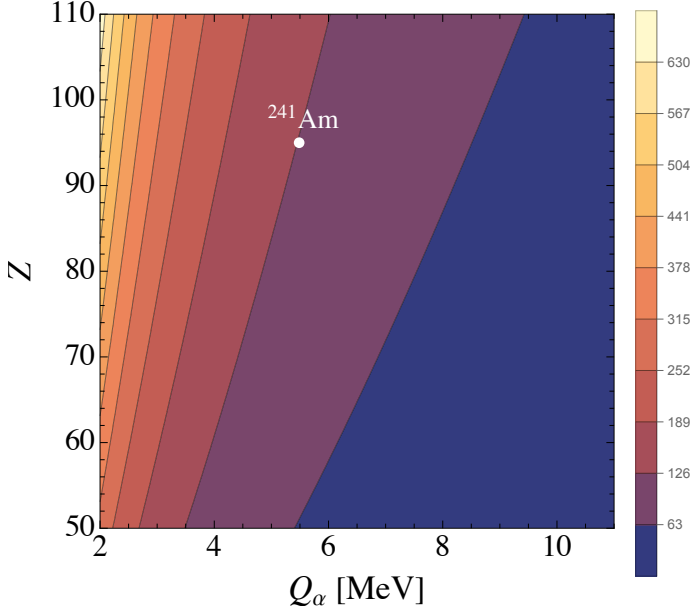


Figure A.3: Contours of  $\hat{T}_{1/2}(0)/T_{1/2}(0)$  in the  $(Q_\alpha, Z)$  plane for  $A = 241$ . The case of  $^{241}\text{Am}$  is indicated by a white dot.

out from  $K$  in Eq. (A.2), while  $R_{\text{well}}$  enters only through  $F(x)$ , which is a constant in the  $x \rightarrow 0$  limit. Therefore, as anticipated at the end of Sect. 3,  $Q_\alpha$  provides the leading contribution compared e.g. to the nuclear potential. Thus one gets

$$\frac{\hat{T}_{1/2}(0)}{T_{1/2}(0)} \approx \hat{K} \approx \frac{\partial K}{\partial Q_\alpha} \hat{Q}_\alpha, \quad (\text{A.4})$$

with

$$\begin{aligned} \hat{Q}_\alpha &\approx 4.23 [A^{2/3} - (A-4)^{2/3} - 4^{2/3}] \text{ MeV} \\ &\approx -4.23 \text{ MeV} \left[ 4^{2/3} - \frac{8}{3A^{1/3}} \right], \end{aligned} \quad (\text{A.5})$$

from Eq. (17). Expanding  $F(x)$  as in Eq. (A.3), our final estimate gives

$$\frac{\hat{T}_{1/2}(0)}{T_{1/2}(0)} \approx 8.45 (Z-2) \left[ 4^{2/3} - \frac{8}{3A^{1/3}} \right] \left( \frac{\text{MeV}}{Q_\alpha} \right)^{3/2}. \quad (\text{A.6})$$

For instance, for the case of the  $\alpha$ -decay of  $^{241}\text{Am}$ , Eq. (A.6) yields  $\hat{T}_{1/2}(0)/T_{1/2}(0) \approx 128$ , while keeping the full  $F(x)$  dependence in  $K$  one gets 125, in excellent agreement with the numerical result in Eq. (22).

Eq. (A.3) also shows that the main  $\theta$ -dependence arises through  $Q_\alpha$  and  $Z$ , with a weaker dependence from  $A$ . In Fig. A.3 we display the contour values of  $\hat{T}_{1/2}(0)/T_{1/2}(0)$  in the  $(Q_\alpha, Z)$  plane, keeping the full  $F(x)$  dependence in  $K$  and setting  $A = 241$ . In fact, for values  $A \gtrsim 100$  relevant for  $\alpha$ -decays, the  $A$  dependence turns out to be rather weak. Hence, we conclude that  $^{241}\text{Am}$  performs rather well in the landscape of possibilities for probing the  $\theta$ -dependence of  $\alpha$ -decay.

## References

- [1] R. D. Peccei, H. R. Quinn, CP Conservation in the Presence of Instantons, *Phys. Rev. Lett.* 38 (1977) 1440–1443. doi:10.1103/PhysRevLett.38.1440.
- [2] R. D. Peccei, H. R. Quinn, Constraints Imposed by CP Conservation in the Presence of Instantons, *Phys. Rev. D* 16 (1977) 1791–1797. doi:10.1103/PhysRevD.16.1791.
- [3] S. Weinberg, A New Light Boson?, *Phys. Rev. Lett.* 40 (1978) 223–226. doi:10.1103/PhysRevLett.40.223.
- [4] F. Wilczek, Problem of Strong  $P$  and  $T$  Invariance in the Presence of Instantons, *Phys. Rev. Lett.* 40 (1978) 279–282. doi:10.1103/PhysRevLett.40.279.
- [5] M. Dine, W. Fischler, The Not So Harmless Axion, *Phys. Lett. B* 120 (1983) 137–141. doi:10.1016/0370-2693(83)90639-1.
- [6] L. F. Abbott, P. Sikivie, A Cosmological Bound on the Invisible Axion, *Phys. Lett. B* 120 (1983) 133–136. doi:10.1016/0370-2693(83)90638-X.
- [7] J. Preskill, M. B. Wise, F. Wilczek, Cosmology of the Invisible Axion, *Phys. Lett. B* 120 (1983) 127–132. doi:10.1016/0370-2693(83)90637-8.
- [8] I. G. Irastorza, J. Redondo, New experimental approaches in the search for axion-like particles, *Prog. Part. Nucl. Phys.* 102 (2018) 89–159. arXiv:1801.08127, doi:10.1016/j.pnpnp.2018.05.003.
- [9] L. Di Luzio, M. Giannotti, E. Nardi, L. Visinelli, The landscape of QCD axion models, *Phys. Rept.* 870 (2020) 1–117. arXiv:2003.01100, doi:10.1016/j.physrep.2020.06.002.
- [10] P. Sikivie, Invisible Axion Search Methods, *Rev. Mod. Phys.* 93 (1) (2021) 015004. arXiv:2003.02206, doi:10.1103/RevModPhys.93.015004.
- [11] P. W. Graham, S. Rajendran, New Observables for Direct Detection of Axion Dark Matter, *Phys. Rev. D* 88 (2013) 035023. arXiv:1306.6088, doi:10.1103/PhysRevD.88.035023.
- [12] D. Budker, P. W. Graham, M. Ledbetter, S. Rajendran, A. Sushkov, Proposal for a Cosmic Axion Spin Precession Experiment (CASPER), *Phys. Rev. X* 4 (2) (2014) 021030. arXiv:1306.6089, doi:10.1103/PhysRevX.4.021030.
- [13] Y. V. Stadnik, V. V. Flambaum, Axion-induced effects in atoms, molecules, and nuclei: Parity nonconservation, anapole moments, electric dipole moments, and spin-gravity and spin-axion momentum couplings, *Phys. Rev. D* 89 (4) (2014) 043522. arXiv:1312.6667, doi:10.1103/PhysRevD.89.043522.
- [14] K. Blum, R. T. D’Agnolo, M. Lisanti, B. R. Safdi, Constraining Axion Dark Matter with Big Bang Nucleosynthesis, *Phys. Lett. B* 737 (2014) 30–33. arXiv:1401.6460, doi:10.1016/j.physletb.2014.07.059.
- [15] C. Abel, et al., Search for Axionlike Dark Matter through Nuclear Spin Precession in Electric and Magnetic Fields, *Phys. Rev. X* 7 (4) (2017) 041034. arXiv:1708.06367, doi:10.1103/PhysRevX.7.041034.
- [16] A. Hook, J. Huang, Probing axions with neutron star inspirals and other stellar processes, *JHEP* 06 (2018) 036. arXiv:1708.08464, doi:10.1007/JHEP06(2018)036.
- [17] T. S. Roussy, et al., Experimental Constraint on Axionlike Particles over Seven Orders of Magnitude in Mass, *Phys. Rev. Lett.* 126 (17) (2021) 171301. arXiv:2006.15787, doi:10.1103/PhysRevLett.126.171301.
- [18] I. Schulthess, et al., New Limit on Axionlike Dark Matter Using Cold Neutrons, *Phys. Rev. Lett.* 129 (19) (2022) 191801. arXiv:2204.01454, doi:10.1103/PhysRevLett.129.191801.
- [19] R. Balkin, J. Serra, K. Springmann, S. Stelzl, A. Weiler, White dwarfs as a probe of light QCD axions arXiv:2211.02661.
- [20] X. Zhang, A. Banerjee, M. Leyser, G. Perez, S. Schiller, D. Budker, D. Antypas, Search for Ultralight Dark Matter with Spectroscopy of Radio-Frequency Atomic Transitions, *Phys. Rev. Lett.* 130 (25) (2023) 251002. arXiv:2212.04413, doi:10.1103/PhysRevLett.130.251002.
- [21] X. Zhang, N. Houston, T. Li, Nuclear decay anomalies as a signature of axion dark matter, *Phys. Rev. D* 108 (7) (2023) L071101. arXiv:2303.09865, doi:10.1103/PhysRevD.108.L071101.
- [22] D. Lee, U.-G. Meißner, K. A. Olive, M. Shifman, T. Vonk,  $\theta$ -dependence of light nuclei and nucleosynthesis, *Phys. Rev. Res.* 2 (3) (2020) 033392. arXiv:2006.12321, doi:10.1103/PhysRevResearch.2.033392.

- [23] S. Pommé, et al., On decay constants and orbital distance to the sun - part ii: beta minus decay, *Metrologia* 54 (1) (2016) 19. doi:10.1088/1681-7575/54/1/19. URL <https://dx.doi.org/10.1088/1681-7575/54/1/19>
- [24] M. Curie, PhD Thesis, Doctoral Dissertation, Sorbonne University, Paris.
- [25] M. H. McDuffie, P. Graham, J. L. Eppel, J. T. Gruenwald, D. Javorsek, D. E. Krause, E. Fischbach, Anomalies in Radioactive Decay Rates: A Bibliography of Measurements and Theory arXiv:2012.00153.
- [26] S. Pommé, et al., On decay constants and orbital distance to the sun - part i: alpha decay, *Metrologia* 54 (1) (2016) 1. doi:10.1088/1681-7575/54/1/1. URL <https://dx.doi.org/10.1088/1681-7575/54/1/1>
- [27] S. Pommé, et al., On decay constants and orbital distance to the sun - part iii: beta plus and electron capture decay, *Metrologia* 54 (1) (2016) 36. doi:10.1088/1681-7575/54/1/36. URL <https://dx.doi.org/10.1088/1681-7575/54/1/36>
- [28] E. Bellotti, C. Broggin, G. Di Carlo, M. Laubenstein, R. Menegazzo, Search for the time dependence of the  $^{137}\text{Cs}$  decay constant, *Phys. Lett. B* 710 (2012) 114–117. arXiv:1202.3662, doi:10.1016/j.physletb.2012.02.083.
- [29] E. Bellotti, C. Broggin, G. Di Carlo, M. Laubenstein, R. Menegazzo, Precise measurement of the  $^{222}\text{Rn}$  half-life: A probe to monitor the stability of radioactivity, *Phys. Lett. B* 743 (2015) 526–530. arXiv:1501.07757, doi:10.1016/j.physletb.2015.03.021.
- [30] E. Bellotti, C. Broggin, G. Di Carlo, M. Laubenstein, R. Menegazzo, M. Pietroni, Search for time modulations in the decay rate of  $^{40}\text{K}$  and  $^{232}\text{Th}$ , *Astropart. Phys.* 61 (2015) 82–87. arXiv:1311.7043, doi:10.1016/j.astropartphys.2014.05.006.
- [31] E. Bellotti, C. Broggin, G. Di Carlo, M. Laubenstein, R. Menegazzo, Search for time modulations in the decay constant of  $^{40}\text{K}$  and  $^{226}\text{Ra}$  at the underground Gran Sasso Laboratory, *Phys. Lett. B* 780 (2018) 61–65. arXiv:1802.09373, doi:10.1016/j.physletb.2018.02.065.
- [32] P. R. Chowdhury, C. Samanta, D. N. Basu, Alpha decay half-lives of new superheavy elements, *Phys. Rev. C* 73 (2006) 014612. arXiv:nucl-th/0507054, doi:10.1103/PhysRevC.73.014612.
- [33] C. Samanta, P. R. Chowdhury, D. N. Basu, Predictions of Alpha Decay Half lives of Heavy and Superheavy Elements, *Nucl. Phys. A* 789 (2007) 142–154. arXiv:nucl-th/0703086, doi:10.1016/j.nuclphysa.2007.04.001.
- [34] M. Sayahi, V. Dehghani, D. Naderi, S. A. Alavi, Prediction of Alpha Decay Half-Lives of  $Z = 118$ –121 Superheavy Nuclei with  $A \leq 300$  by Using the Double-Folding Potential, *Z. Naturforsch. A* 74 (7) (2019) 551–560. doi:10.1515/zna-2019-0008.
- [35] G. Gamow, Zur Quantentheorie des Atomkernes, *Z. Phys.* 51 (1928) 204–212. doi:10.1007/BF01343196.
- [36] R. W. Gurney, E. U. Condon, Quantum Mechanics and Radioactive Disintegration, *Phys. Rev.* 33 (1929) 127–140. doi:10.1103/PhysRev.33.127.
- [37] B. R. Holstein, Understanding alpha decay, *Am. J. Phys.* 64 (8) (1996) 1061–1071. doi:10.1119/1.18308.
- [38] G. R. Satchler, W. G. Love, Folding model potentials from realistic interactions for heavy-ion scattering, *Phys. Rept.* 55 (1979) 183–254. doi:10.1016/0370-1573(79)90081-4.
- [39] G. Bertsch, J. Borysowicz, H. McManus, W. G. Love, Interactions for inelastic scattering derived from realistic potentials, *Nucl. Phys. A* 284 (1977) 399–419. doi:10.1016/0375-9474(77)90392-X.
- [40] A. M. Kobos, B. A. Brown, R. Lindsay, G. R. Satchler, Folding-model analysis of elastic and inelastic alpha-particle scattering using a density-dependent force, *Nucl. Phys. A* 425 (1984) 205–232. doi:10.1016/0375-9474(84)90073-3.
- [41] H. J. Gils, Density dependent effective interactions in double-folding model analyses of elastic  $\alpha$ -particle scattering, *Nucl. Phys. A* 473 (1987) 111–128. doi:10.1016/0375-9474(87)90157-6.
- [42] N. Anantaraman, H. Toki, G. F. Bertsch, An effective interaction for inelastic scattering derived from the Paris potential, *Nucl. Phys. A* 398 (1983) 269–278. doi:10.1016/0375-9474(83)90487-6.
- [43] C. Abel, et al., Measurement of the Permanent Electric Dipole Moment of the Neutron, *Phys. Rev. Lett.* 124 (8) (2020) 081803. arXiv:2001.11966, doi:10.1103/PhysRevLett.124.081803.
- [44] L. Ubaldi, Effects of theta on the deuteron binding energy and the triple-alpha process, *Phys. Rev. D* 81 (2010) 025011. arXiv:0811.1599, doi:10.1103/PhysRevD.81.025011.
- [45] H. Leutwyler, A. V. Smilga, Spectrum of Dirac operator and role of winding number in QCD, *Phys. Rev. D* 46 (1992) 5607–5632. doi:10.1103/PhysRevD.46.5607.
- [46] R. Brower, S. Chandrasekharan, J. W. Negele, U. J. Wiese, QCD at fixed topology, *Phys. Lett. B* 560 (2003) 64–74. arXiv:hep-lat/0302005, doi:10.1016/S0370-2693(03)00369-1.
- [47] N. R. Acharya, F.-K. Guo, M. Mai, U.-G. Meißner,  $\theta$ -dependence of the lightest meson resonances in QCD, *Phys. Rev. D* 92 (2015) 054023. arXiv:1507.08570, doi:10.1103/PhysRevD.92.054023.
- [48] R. J. Furnstahl, B. D. Serot, Parameter counting in relativistic mean field models, *Nucl. Phys. A* 671 (2000) 447–460. arXiv:nucl-th/9911019, doi:10.1016/S0375-9474(99)00839-8.
- [49] J. F. Donoghue, Sigma exchange in the nuclear force and effective field theory, *Phys. Lett. B* 643 (2006) 165–170. arXiv:nucl-th/0602074, doi:10.1016/j.physletb.2006.10.033.
- [50] T. Damour, J. F. Donoghue, Constraints on the variability of quark masses from nuclear binding, *Phys. Rev. D* 78 (2008) 014014. arXiv:0712.2968, doi:10.1103/PhysRevD.78.014014.
- [51] J. F. Donoghue, The Nuclear central force in the chiral limit, *Phys. Rev. C* 74 (2006) 024002. arXiv:nucl-th/0603016, doi:10.1103/PhysRevC.74.024002.
- [52] C. F. V. Weizsacker, Zur Theorie der Kernmassen, *Z. Phys.* 96 (1935) 431–458. doi:10.1007/BF01337700.
- [53] U.-G. Meißner, B. C. Metsch, H. Meyer, The electromagnetic fine-structure constant in primordial nucleosynthesis revisited, *Eur. Phys. J. A* 59 (10) (2023) 223. arXiv:2305.15849, doi:10.1140/epja/s10050-023-01131-3.
- [54] C. O’Hare, cajohare/axionlimits: Axionlimits, <https://cajohare.github.io/AxionLimits/> (Jul. 2020). doi:10.5281/zenodo.3932430.
- [55] G. Lucente, L. Mastrototaro, P. Carena, L. Di Luzio, M. Giannotti, A. Mirizzi, Axion signatures from supernova explosions through the nucleon electric-dipole portal, *Phys. Rev. D* 105 (12) (2022) 123020. arXiv:2203.15812, doi:10.1103/PhysRevD.105.123020.
- [56] A. Hook, Solving the Hierarchy Problem Discretely, *Phys. Rev. Lett.* 120 (26) (2018) 261802. arXiv:1802.10093, doi:10.1103/PhysRevLett.120.261802.
- [57] L. Di Luzio, B. Gavela, P. Quilez, A. Ringwald, An even lighter QCD axion, *JHEP* 05 (2021) 184. arXiv:2102.00012, doi:10.1007/JHEP05(2021)184.
- [58] L. Di Luzio, B. Gavela, P. Quilez, A. Ringwald, Dark matter from an even lighter QCD axion: trapped misalignment, *JCAP* 10 (2021) 001. arXiv:2102.01082, doi:10.1088/1475-7516/2021/10/001.
- [59] A. Banerjee, J. Eby, G. Perez, From axion quality and naturalness problems to a high-quality ZN QCD relaxation, *Phys. Rev. D* 107 (11) (2023) 115011. arXiv:2210.05690, doi:10.1103/PhysRevD.107.115011.